PHYSICAL REVIEW D VOLUME 39, NUMBER 1 1 JANUARY 1989

Geometrical branching model: Phenomenology with jets

Wei R. Chen and Rudolph C. Hwa
Institute of Theoretical Science and Department of Physics, University of Oregon, Eugene, Oregon 97403
(Received 26 October 1987; revised manuscript received 2 May 1988)

The geometrical branching model with jets is used to analyze the data on $\sigma_{el}, \sigma_{tot}, \langle n \rangle$, and the higher moments of particle multiplicity in hadron-hadron collisions at all available energies. The eikonal formalism is used as the framework to combine the soft and hard components of the multiparticle production process. The soft component of the eikonal function is assumed to be geometrical scaling even in the presence of the hard component. We show in the context of the model that the geometrical size of a hadron ceases to increase in the energy region of the CERN S$p\bar{p}$S collider. The production of jets is shown to be responsible not only for the continued increase of the inelastic cross section, but also for the breaking of the Koba-Nielson-Olesen scaling.

I. INTRODUCTION

This is the third in a series of papers on the geometrical branching model for multiparticle production in hadron-hadron collision at high energy. The first is on combining geometrical scaling and Furry branching in a model that yields Koba-Nielson-Olesen (KNO) scaling.[1] It gives a good description of the multiplicity distribution in the CERN ISR energy range $20 \leq \sqrt{s} \leq 65$ GeV. The second in the series extends the geometrical branching model (GBM) in order to treat the problem of forward-backward multiplicity correlation on the one hand, and on the other, generalizes the model to higher energies, when the production of jets becomes important.[2] In this third paper we carry out the phenomenology of the GBM with jets in the CERN S$p\bar{p}$S energy range $200 \leq \sqrt{s} \leq 900$ GeV. In so doing we shall show how nearly all major features of high-energy collisions, ranging from elastic cross sections to parton decay functions, are to be amalgamated in the formation of one unified picture of strong interaction at long and short distances.

Minimum-bias physics in hadronic collisions is complicated because it involves many strands of strong-interaction physics that cannot be decoupled. While it is possible, indeed sometimes necessary, to focus on one issue at a time in some selected areas of investigation, a general description of hadronic processes at high energy must confront as many issues as possible simultaneously, and succeed in incorporating all the major features. Although economy in the description is important, fundamentality in terms of basic constituents and their interactions should not be the overriding criterion, when the physical phenomena to be described involve length scales much larger than those of the constituents. In other words, instead of searching for a fundamental theory of hadronic processes, a more fruitful line of investigation should be directed at the discovery of a general framework in which all the phenomenological properties of those processes can be described. Such a framework should, for example, give explicit credence to the picture that hadrons are geometrically extended objects consisting of pointlike constituents. In collisions they produce particles so numerous that statistical behavior independent of energy should have a natural expression in the framework, yet the energy dependence of elastic and total cross sections should also be the prominent features that have their rightful places in the description. We attempt in this series of papers to construct just such a framework; in this paper we cement the construction with phenomenology and show that the whole scheme is empirically realistic over the entire energy range accessible to data.

Since the GBM is already first described in Ref. 1 and then further reviewed and extended in Ref. 2, we shall not reproduce all the relevant equations here yet another time. In the following we shall refer to the equations in Ref. 2 with the prefix II.

II. CROSS SECTIONS WITH JETS

Let us briefly recall the key issue involved in the GBM with jets. Without jets the GBM successfully described KNO scaling for $\sqrt{s} < 100$ GeV (Ref. 1). The breaking of the KNO scaling for $\sqrt{s} > 100$ GeV is attributed to the production of jets, which also breaks geometrical scaling.[2] The principal objection to an identification of such jets with the low-E_T jets of UA1 (Ref. 3) called minijets, is the arbitrariness in the algorithm adopted in the experiment to define a jet. The mechanism that breaks KNO and geometrical scalings must involve a type of process that can only be described in a probabilistic sense, since KNO and geometrical scalings are themselves notions based on the statistical properties of many observed events. Thus a definition of the hard component that involves jet production, if probabilistic in its definition, cannot be translated into an algorithm for jet identification from even to event in an experiment. In short, the jets of concern to the GBM are not the minijets of UA1.

The central point in our separation of the inelastic cross section into a soft and a hard component is that we define what a soft component is. This is to be contrasted from an experimental definition of what a hard component is. Because of the unitarity complication the two

definitions are not complementary; hence, they define two different separations. Our definition is based on theoretical reasoning, while the other is based on experimental expediency. In our reasoning we argue that geometrical scaling would have continued to be valid at higher energies, if it were not for the emergence of nongeometrical absorptive processes which can no longer be ignored above a threshold, say, around 100 GeV. Large-angle scatterings of pointlike partons with high momenta are such processes. Thus we define the soft component to be the geometrical scaling part that is continued from below to above that threshold, but subject to a nonscaling suppression factor due to the requirement that there be no jets in the soft component.

More precisely, we assume that the soft and hard components are additive in the eikonal function

$$\Omega(s,b)=\Omega_0(s,b)+\Omega_1(s,b) . \tag{2.1}$$

The soft component Ω_0 possesses the geometrical scaling property even when $\sqrt{s}$ is above the jet threshold, i.e., $\Omega_0(s,b)=\Omega_0(R)$, where R is the scaled impact parameter: $R=b/b_0(s)$. Separating the inelastic cross section also into two components,

$$\sigma_{\rm in}=\sigma^s+\sigma^h , \tag{2.2}$$

we have [II-(4.7)]

$$\sigma^s=\pi\int_0^\infty db^2(1-e^{-2\Omega_0(R)})e^{-2\Omega_1(s,b)} \tag{2.3}$$

and [II-(4.8)]

$$\sigma^h=\pi\int_0^\infty db^2(1-e^{-2\Omega_1(s,b)}) . \tag{2.4}$$

Since $2\Omega_1(s,b)$ has the interpretation of being the probability of having one hard collision among the partons of the colliding hadrons,[4] it is proportional to an appropriately defined $\sigma_{\rm jet}$, as well as to $\Omega_0(R)$ on geometrical grounds. Thus, we have [II-(4.14)]

$$\Omega_1(s,b)=\Omega_0(R)\chi(s) , \tag{2.5}$$

where

$$\chi(s)=\sigma_{\rm jet}(s)\left[2\sigma_0(s)\int dR^2\Omega_0(R)\right]^{-1} . \tag{2.6}$$

We use $\sigma_{\rm jet}$ here without first specifying the criteria of what a jet is. $\sigma_0(s)$ is the "geometrical" cross section $\pi b_0^2(s)$.

An important point to note about the foregoing is that there are two unknown quantities with the dimension of cross section: $\sigma_0(s)$ and $\sigma_{\rm jet}(s)$, which are both dependent on s. Geometrical scaling[5] is a concept that involves no scale (specifically, $\sigma_{\rm el}/\sigma_{\rm tot}=0.17$), so it cannot determine σ_0 or $\sigma_{\rm jet}$. It is here that we use phenomenology to connect the scaling concept with the quantities that manifestly depend on the scale, i.e., scaling violation. The necessity for a phenomenological input at this point is unavoidable in any theory in which a scale must be introduced. We determine $\sigma_0(s)$ and $\sigma_{\rm jet}(s)$ by the observed $\sigma_{\rm el}(s)$ and $\sigma_{\rm tot}(s)$ at *one* value of s where the ratio $\sigma_{\rm el}/\sigma_{\rm tot}$ is significantly different from 0.17. Thus the breaking of geometrical scaling is related to the nonvanishing of $\sigma_{\rm jet}(s)$. By the usual procedure in perturbative QCD, the magnitude of $\sigma_{\rm jet}(s)$ can be related to a single parameter $k_T^{\rm min}$, the cutoff in the parton transverse momentum. Just as $\Lambda_{\rm QCD}$ determines the Q^2 dependence of the running coupling constant, if perturbative QCD provides the correct description, so also should the scale parameter $k_T^{\rm min}$ determine the s dependence of $\sigma_{\rm tot}(s)$, if our model is to be successful. If $k_T^{\rm min}$ must be varied as a function of s, then $k_T^{\rm min}$ would lose its significance in setting a scale, and the model obviously would have no predictive power.

The phenomenology proceeds as follows. First, we recall the cross sections in the eikonal formalism

$$\sigma_{\rm el}=\sigma_0\int_0^\infty dR^2(1-e^{-\Omega(s,R)})^2 , \tag{2.7}$$

$$\sigma_{\rm in}=\sigma_0\int_0^\infty dR^2(1-e^{-2\Omega(s,R)}) , \tag{2.8}$$

$$\sigma_{\rm tot}=2\sigma_0\int_0^\infty dR^2(1-e^{-\Omega(s,R)}) \tag{2.9}$$

which differ from II-(4.1)–II-(4.3) only in that the substitution $b=b_0(s)R$ has been made and $\sigma_0=\pi b_0^2(s)$ used. Putting (2.1), (2.5), and (2.6) in (2.7) and (2.9) results in an explicit simultaneous dependence of $\sigma_{\rm el}$ and $\sigma_{\rm tot}$ on σ_0 and $\sigma_{\rm jet}$ through the function $\Omega_0(R)$. The latter is a known phenomenological quantity. We use the Gaussian form[6]

$$1-e^{-\Omega_0(R)}=0.71e^{-1.17R^2} . \tag{2.10}$$

The parameters in (2.10) have been fixed by us to fit $\sigma_{\rm el}$ and $\sigma_{\rm tot}$ in the CERN ISR energy range. It differs from our earlier parametrization[1]

$$\Omega_0(R)=1.4e^{-1.62R^2} \tag{2.11}$$

in a way that does not affect our results in Ref. 1, but provides a better description of $d\sigma/dt$ within the diffraction peak. Either parametrization is a result of the geometrical description of pp elastic scattering and $\sigma_{\rm tot}$ at $\sqrt{s}\lesssim 65$ GeV. To continue using the same parametrization of $\Omega_0(R)$ at higher energies is the essence of our procedure of extending geometrical scaling into a region where $\Omega_1(s,R)$ is not zero, and thereby defining the soft component of Ω.

The result of our calculation of $\sigma_{\rm el}$ and $\sigma_{\rm tot}$ in terms of σ_0 and $\sigma_{\rm jet}$ is shown by the dashed and dotted lines in Fig. 1. We have plotted $\sigma_{\rm tot}$ vs $\sigma_{\rm el}/\sigma_{\rm tot}$ so that the data points[7] from ISR line up along a constant $\sigma_{\rm el}/\sigma_{\rm tot}$ value of 0.175. That is the empirical evidence for geometrical scaling and corresponds to $\sigma_{\rm jet}=0$ in our model. At higher energy there is only one published data point at 540 GeV from UA4 (Ref. 8), as shown by the solid circle in Fig. 1. The open squares are the extrapolated results of Carlson[9] at other S$p\bar{p}$S energies. We use the 540-GeV data to fix the values

$$\sigma_0(540)=40\ {\rm mb},\quad \sigma_{\rm jet}(540)=24\ {\rm mb} . \tag{2.12}$$

At other energies the question we ask is whether (2.12) supplies all the information that we need, viz., $\sigma_0(s)$ constant at 40 mb for $\sqrt{s}\geq 200$ GeV and $\sigma_{\rm jet}(s)$ being determined by a fixed $k_T^{\rm min}$ obtained from (2.12). The constancy of σ_0 in the S$p\bar{p}$S range is hinted by the data in Fig. 1; the constancy of $k_T^{\rm min}$ remains to be checked.

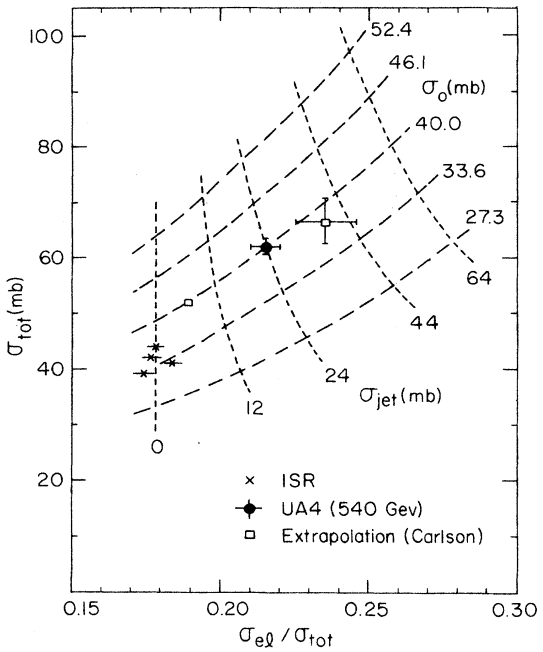

FIG. 1. A plot of σ_{tot} vs σ_{el}/σ_{tot}. The dashed lines are for different constant values of $\sigma_0=\pi b_0^2(s)$; the dotted lines are for different constant values of σ_{jet}. Data points are from Refs. 7–9.

Following the usual procedure in perturbative QCD for calculating σ_{jet} due to the hard scattering of partons, as outlined in Ref. 2, we have [II-(4.30)]

$$\sigma_{jet}(s)=\int \frac{dx_1}{x_1}\frac{dx_2}{x_2}\int_{-z_0}^{z_0}\frac{dz}{2}F(x_1)F(x_2)\frac{d\hat{\sigma}}{dz}\ , \tag{2.13}$$

where

$$z_0=(1-4k_T^{\min 2}/x_1x_2s)^{1/2}\ . \tag{2.14}$$

Using the effective parton distribution[10]

$$F(x)=G(x)+\tfrac{4}{9}[Q(x)+\bar{Q}(x)] \tag{2.15}$$

for the gluon and quark distributions, $G(x)$ and $Q(x)$, respectively, we adopt the UA1 parametrization[11]

$$F(x)=6.2e^{-9.5x}\ . \tag{2.16}$$

The hard-scattering differential cross section is

$$\frac{d\hat{\sigma}}{dz}=\frac{9\pi\alpha_s^2(Q^2)}{16x_1x_2s}\frac{(3+z^2)^3}{(1-z^2)^2} \tag{2.17}$$

for which we have used what is appropriate for the gluon scattering only. We have used $Q^2=p_T^2/4$ for the virtuality in (2.17). From the above equations it is evident that $\sigma_{jet}(s)$ is completely determined by $k_T^{\min}$. The value of 24 mb for $\sigma_{jet}(540)$ corresponds to

$$k_T^{\min}=2.7\ \text{GeV}\ , \tag{2.18}$$

a value which is large enough to render the application of perturbative QCD not unreasonable, although a somewhat larger value would have been even easier to justify.

To examine the question whether a constant $k_T^{\min}$ suffices for all energies, we have calculated σ_{tot} and σ_{el}/σ_{tot} in the S$p\bar{p}$S range assuming constant σ_0 and $k_T^{\min}$ and obtained the results shown in Figs. 2 and 3. Our calculated results on cross sections are not sensitive to the choice of Q^2. For instance, using $Q^2=-t=\frac{1}{2}x_1x_2s(1-\cos\theta)$, we can reproduce the curves of σ_{tot} and σ_{el}/σ_{tot} in Figs. 2 and 3, with the corresponding $k_T^{\min}$ being 2.1 GeV. Note that in Fig. 2 the solid curve for σ_{tot} goes through the S$p\bar{p}$S as well as the cosmic-ray data points, but the dashed curve for σ_{jet} diverges badly, a clear demonstration of the necessity for unitarization.[4] Figure 3 vividly exhibits the violation of geometrical scaling above 100 GeV. A corollary to this analysis is that if $k_T^{\min}$ is fixed at 2.7 GeV, then only an s-independent $\sigma_0(s)$ can fit the cross-section data throughout the S$p\bar{p}$S energies. The behavior of $\sigma_0(s)$ for $\sqrt{s}>20$ GeV is shown in Fig. 4. In the ISR energy range $\sigma_0(s)$ is specified by the observed $\sigma_{in}(s)$; in the S$p\bar{p}$S range it is fixed at 40 mb. The two are joined by hand in the transition region using a smooth curve, the precise shape of which has no significance. In the same figure we also show $\sigma_{in}(s)$ and $\sigma^s(s)$, as given in (2.2)–(2.4). The decrease of σ^s with increasing s is due to the suppression factor $\exp(-2\Omega_1)$ in (2.3), which expresses the diminishing probability that an event contains no jets at high s.

The implication of a constant $\sigma_0(s)$ is quite interesting. In the ISR energy range, geometrical scaling means that, as s increases, a hadron increases in size, while its opaqueness at a fixed b also increases in such a way that $\Omega(s,b)$ depends only on the scaled variable R. The increase in size is given by the s dependence of $\sigma_{in}(s)$. As s further increases into the S$p\bar{p}$S range, the observed σ_{in} continues to increase, but σ_0 reaches an asymptote; σ^s decreases, while σ^h picks up the increase. This seems physi-

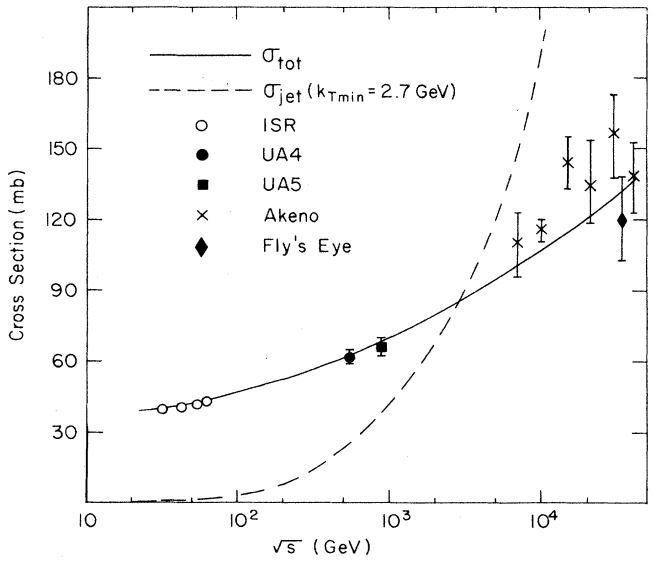

FIG. 2. Cross sections versus c.m. energy $\sqrt{s}$. The solid curve is σ_{tot}, calculated from (2.1) and (2.9). The dashed curve is σ_{jet} calculated with $k_T^{\min}=2.7$ GeV. Data points beyond S$p\bar{p}$S region are from cosmic-ray experiments (Ref. 4).

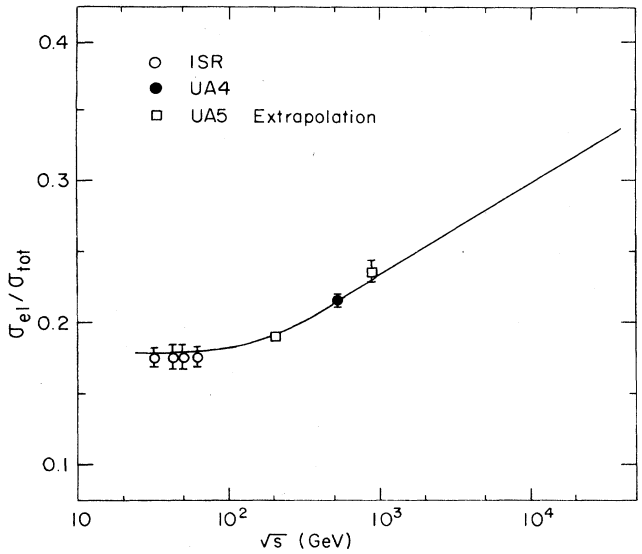

FIG. 3. σ_{el}/σ_{tot} vs c.m. energy $\sqrt{s}$. Data points are from Refs. 7–9.

cally reasonable, if we identify σ_0 with the geometrical size $\pi b_0^2(s)$, and σ^h with the part of the cross section arising from the added absorption due to hard scattering between pointlike partons. It is intuitively sensible to expect the geometrical size of a hadron not to increase with energy forever. The preliminary result from UA1 on Bose-Einstein correlations between charged pions appear to indicate that the transverse size of a proton ceases to increase with s at the $S\bar{p}pS$ (Ref. 12).

We emphasize the importance of recognizing that the value of $k_T^{\min}$ in (2.18) is an inferred result from phenomenology, just as Λ_{QCD} is in the experiments on QCD coupling, and that it is not set arbitrarily to define a jet. Indeed, (2.18) is meaningful only in the context of the lowest-order perturbative calculation in QCD. An improvement of that calculation can undoubtedly change the value of $k_T^{\min}$, but what will not change in the GBM is the value of σ_{jet} in (2.12) determined from experimental data. Thus $k_T^{\min}$ has no strong connection with an experimental $p_{T_{cut}}$ for the definition of an observable jet, unless the lowest-order perturbative QCD is the complete theoretical description of jet production with zero contributions from the higher orders and higher twists.

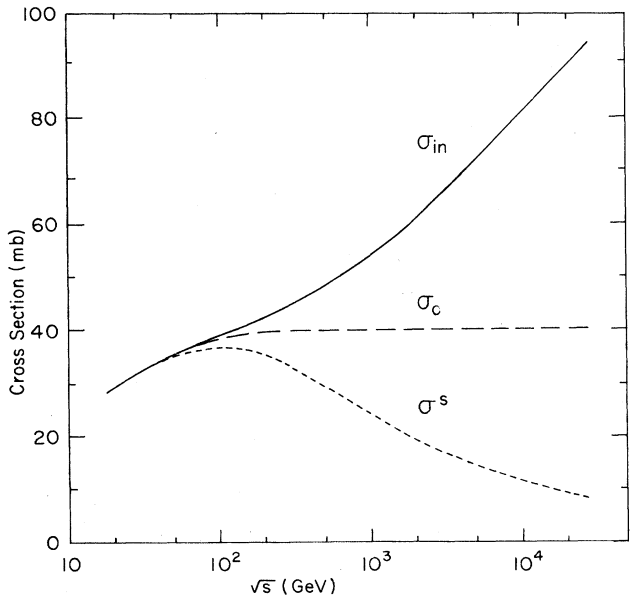

FIG. 4. The solid line is the total inelastic cross section; the dashed line is $\sigma_0=\pi b_0^2(s)$. The dotted line is σ^s calculated from (2.3), using 2.7 GeV as the p_T cutoff in Ω_1.

In Figs. 2–4 we have plotted the calculated curves to $\sqrt{s}=4\times10^4$ GeV, as determined according to our prescription for computing $\sigma_{jet}(s)$ summarized in (2.13)–(2.18). The purpose is merely to indicate what the GBM plus jets (in the approximation adopted without further modification) would predict, thereby showing the relative sizes of σ_{in}, σ_0, and σ^s in Fig. 4. We must, however, stress that the extrapolation to higher energy above 1 TeV should not be taken seriously in any quantitative way. There are many approximations in our treatment of the hard-scattering part that are inadequate for handling the higher-energy regime. To mention a few, they are (A) the UA1 parametrizations in (2.16) are inaccurate without scaling violation, (B) an effective parton distribution may be a poor approximation, (C) quark and gluon channels may have to be treated separately, (D) multiple production of minijets may be important, (E) shadowing at small x may have to be considered, and (F) the recent discovery of ρ (the ratio of real to imaginary parts of the elastic scattering amplitude) may require a complex Ω for a better treatment. The formalism developed in this paper is meant only for phenomenology in the CERN collider energy region, and the purpose is to demonstrate that the GBM with jets can describe the various features in the data at those energies.

III. MULTIPLICITY DISTRIBUTION WITH JETS

As we have discussed before, the GBM without jets is designed to give the KNO-scaling multiplicity distribution, while the model with jets is supposed to account for the violation of KNO scaling. Now, we must demonstrate that the jets introduced in the previous section, which are responsible for the breaking of the geometrical scaling, can indeed fulfill that role.

We recall that without jets the multiplicity distribution in the GBM is [II-(2.14)]

$$P_n=\int_0^\infty dR^2 g(R) F_n^{k(R)} , \tag{3.1}$$

where $g(R)$ is the scaling overlap function [II-(2.13)]:

$$g(R)=1-\exp[-2\Omega(R)] . \tag{3.2}$$

$F_n^{k(R)}$ is the Furry branching distribution [II-(2.10)]:

$$F_n^k(w)=\frac{\Gamma(n)}{\Gamma(k)\Gamma(n-k+1)}\left[\frac{1}{w}\right]^k\left[1-\frac{1}{w}\right]^{n-k} , \tag{3.3}$$

where $w=\bar{n}/k$. When jets are included, the expression for P_n becomes [II-(4.15)]

$$P_n=\sigma_{\rm in}^{-1}(\sigma^s P_n^s+\sigma^h P_n^h)\ , \tag{3.4}$$

where [II-(4.16) and II-(4.17)]

$$\sigma^s P_n^s=\sigma_0\int_0^\infty dR^2(1-e^{-2\Omega_0(R)})e^{-2\Omega_1(s,R)}F_n^{k(R)}(w)\ , \tag{3.5}$$

$$\sigma^h P_n^h=\sigma_0\int_0^\infty dR^2(1-e^{-2\Omega_1(s,R)})H_n(s,R)\ . \tag{3.6}$$

Note that $\Omega(R)$ in (3.2) is replaced by the equivalent $\Omega_0(R)$ in (3.5). The multiplicity distribution of the hard component at R is [II-(4.22)]

$$H_n(s,R)=\frac{1}{\sigma_{\rm jet}}\int\frac{dx_1}{x_1}\frac{dx_2}{x_2}F(x_1)F(x_2)\times\int_{-z_0}^{z_0}\frac{dz}{2}\frac{d\hat{\sigma}}{dz}\sum_{ljm}\delta_{n,l+j+m}F_l^k\Phi_j\Psi_m\ , \tag{3.7}$$

where Φ_j is the multiplicity distribution of a jet fragmenting into j particles, and Ψ_m is the distribution associated with the initial-state bremsstrahlung into m particles. Since Ψ_m is not known well, we shall assume that it is the same as Φ_j, and adopt the following form for both:

$$\Phi_j=\Psi_j=\frac{K^K}{\bar{j}\Gamma(K)}(j/\bar{j})^{K-1}e^{-Kj/\bar{j}} \tag{3.8}$$

which is a form suggested by the phenomenology of the quark decay function in e^+e^- annihilation.[13] In Ref. 13 the empirical value for K is 12, which is what we shall use in the following. We assume that the average multiplicity $\bar{j}$ in a jet behaves as

$$\bar{j}=\alpha\ln\hat{Q}^2+\beta\ln^2\hat{Q}^2\ , \tag{3.9}$$

where $\hat{Q}$ is in units of GeV, and α and β are parameters to be adjusted to fit the multiplicity data. $\hat{Q}$ is the parton momentum transfer

$$\hat{Q}^2=\tfrac{1}{2}x_1x_2s(1-\cos\theta)\ . \tag{3.10}$$

From (3.4) we can calculate the multiplicity moments

$$\langle n^q\rangle=\sigma_{\rm in}^{-1}(\sigma^s\langle n^q\rangle_s+\sigma^h\langle n^q\rangle_h)\ , \tag{3.11}$$

where

$$\langle n^q\rangle_{s,h}=\sum_n n^q P_n^{s,h}\ . \tag{3.12}$$

In view of (3.5) and (3.6) we have

$$\langle n^q\rangle_{s,h}=\frac{\sigma_0}{\sigma^{s,h}}\int_0^\infty dR^2 g_{s,h}^q(s,R)\overline{n_{s,h}^q}(s,R)\ , \tag{3.13}$$

where

$$g_s(s,R)=(1-e^{-2\Omega_0(R)})e^{-2\Omega_1(s,R)}\ , \tag{3.14}$$

$$g_h(s,R)=1-e^{-2\Omega_1(s,R)}\ , \tag{3.15}$$

$$\overline{n_s^q}(s,R)=\sum_n n^q F_n^{k(R)}(w)\ , \tag{3.16}$$

$$\overline{n_h^q}(s,R)=\sum_n n^q H_n(s,R)\ . \tag{3.17}$$

In Ref. 1 the R dependences of $\bar{n}(s,R)$ and $k(s,R)$ are specified by the same function $h(R)$; now at higher s we continue to use $h(R)$ in adherence to our basic point that the geometrical aspect of the problem is unaltered by the introduction of jets. Then we have for the first moment of the soft component (with subscript s suppressed)

$$\bar{n}(s,R)=N(s)h(R)\ , \tag{3.18}$$

$$\bar{k}(s,R)=K(s)h(R)\ . \tag{3.19}$$

Note that $N(s)$ and $K(s)$ are no longer the same as the corresponding quantities in Ref. 1 because of the s dependence in $g_s(s,R)$; nevertheless, the evolution parameter w is

$$w=\frac{\bar{n}(s,R)}{\bar{k}(s,R)}=\frac{N(s)}{K(s)} \tag{3.20}$$

which is related to $N(s)$ as before:[14]

$$w=1+0.114N(s)\ . \tag{3.21}$$

The function $h(R)$ was parametrized previously[1] by

$$h(R)=h_0\Omega^\gamma(R)\ , \tag{3.22}$$

where $\gamma=0.3\pm0.05$. Very recently, we have found a parameter-free description of $h(R)$ that has the form[15]

$$h(R)=\Omega_0(R)\left[(1-e^{-2\Omega_0(R)})\int dR^2\Omega_0(R)\right]^{-1}\ . \tag{3.23}$$

The difference between the phenomenological consequences of the two forms is negligible.

The description of the formalism is now complete. To carry out the calculation requires information on the parameters α and β in (3.9) and on $N(s)$ in (3.18). Unlike the situation in Ref. 1, $N(s)$ is now inequivalent to the observable average multiplicity $\langle n\rangle$, not even its soft component $\langle n\rangle_s$, because of the $e^{-2\Omega_1}$ factor due to hard scattering. We are therefore forced to use the data on the multiplicity moments C_q,

$$C_q=\langle n^q\rangle/\langle n\rangle^q \tag{3.24}$$

at one energy, specifically at $\sqrt{s}=540$ GeV, to determine the three parameters. By fitting the experimental values[16] of $\langle n\rangle$ and C_2 to C_5, we obtain

$$\alpha=0.34\pm0.02,\quad \beta=0.37\pm0.02\ , \tag{3.25}$$

$$N(540)=23.4\pm0.5\ . \tag{3.26}$$

This value of $N(s)$ at 540 GeV lies on a straight-line extrapolation from the ISR values, so we adopt the formula[17]

$$N(s)=-5.13+2.27\ln s \tag{3.27}$$

for all s in units of GeV^2. We then calculate $\langle n\rangle$ and the moments C_q for all s, obtaining the results shown in Figs. 5 and 6; they agree well with the data at all energies.

Some discussion seems appropriate here to explain the results and what has been done to achieve them. One

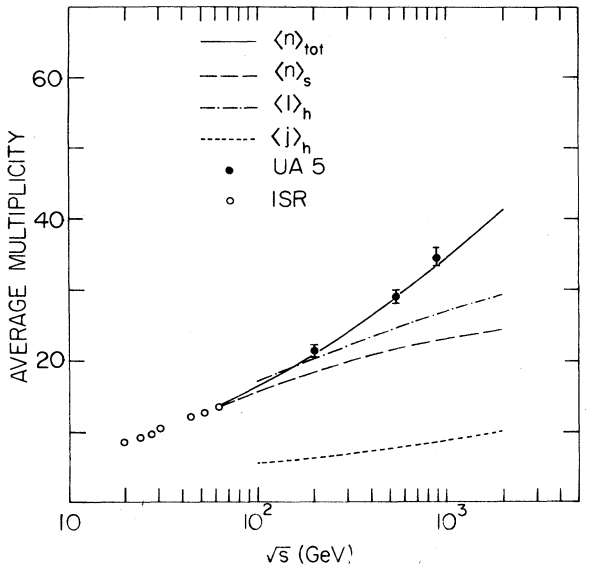

FIG. 5. The solid line is the total average multiplicity. The dashed line is $\langle n \rangle$ in the soft component. The dash-dotted line is the average multiplicity of particles with low p_T produced in the hard processes. The dotted line is the average multiplicity of particles produced in jets. Data are from Refs. 7 and 16.

may naively think that if the data points at 540 GeV in Fig. 6 are fitted, the resultant smooth curves passing through all the other data points as 200 and 900 GeV are easy and natural to obtain. Actually, that is not the case. It is only when we used $\bar{j}$ as expressed in (3.9) and $\hat{Q}^2$ as in (3.10) that we could achieve the fit. When we tried

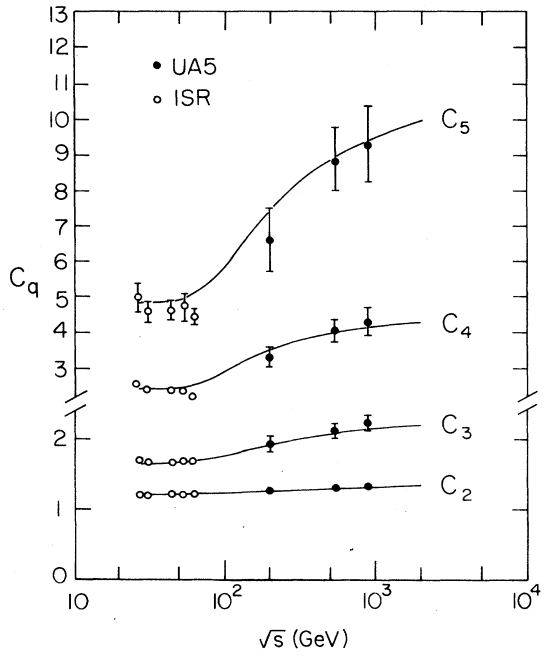

FIG. 6. Normalized moments of multiplicity distribution. Solid lines are calculated results. Data points are from Ref. 16.

other forms, the higher moments C_4 and C_5 developed oscillatory behaviors. The phenomenon has to do with adding two multiplicity distributions as specified in (3.4); the resultant distribution need not be smooth (i.e., without bumps at high n). Depending on the weights at various energies, the degree of dominance of the hard component may affect C_4 and C_5 in such a way that they can temporarily become smaller with increasing energy until the hard component itself begins to develop larger fluctuation due to larger virtuality smearing. We are not certain how to interpret the necessity of the forms in (3.9) and (3.10) in order to achieve the fit. The dependence of $\bar{j}$ and $\hat{Q}^2$ seems reasonable, although we have no precise criteria for that assessment. The minijets are mainly due to gluon large-angle scatterings at $\hat{Q}^2$ where our theoretical and experimental knowledge is not reliable. The proper form for the virtuality in hadronic collisions is known to be not unique and controversial. Our general view on the phenomenology done here is that low-E_T jets are not hard enough to enjoy clean theoretical description; the approximation made here in the adoption of the forms (3.9) and (3.10) crudely summarizes the unknowns about the semihard subprocess. They are not the essence of the GBM. What we can claim is that GBM with jets, made precise in Eqs. (3.1)–(3.7), can produce a fit of the multiplicity distribution data, if the hard component can be described by (3.8)–(3.10) with the parameters specified in (3.25). While the latter are not unreasonable, we have only shown that the GBM with jets can possibly fit the data. To be convincing that it is a successful model, we must test the predictions on some other features of multiparticle production. That will be done in connection with the average transverse momentum in the following paper.

In Fig. 5 the different components of $\langle n \rangle$ are also shown. $\langle l \rangle_h$ signifies the low-p_T multiplicity in the hard component, arising from the soft interactions among the residual partons in conjunction with the hard interaction of one pair of partons. $\langle j \rangle_h$ is the mean jet multiplicity, as well as in the initial-state bremsstrahlung not necessarily at large angles, smeared over virtuality and averaged over impact parameter. Note that the solid curve for $\langle n \rangle$ in Fig. 5 goes through the data points at 200 and 900 GeV, the one at 540 GeV being fitted. The extrapolation to higher energies is meant mainly to show the importance of the jet contribution, even though our consideration of at most only one hard scattering in a collision is likely to be unrealistic at extremely high energies. Note also that the average multiplicity in the hard component, $\langle n \rangle_h = \langle l \rangle_h + 2\langle j \rangle_h$, is larger than that in the soft component $\langle n \rangle_s$, even at $\sqrt{s} \approx 100$ GeV, when $\sigma_{\text{jet}} \approx 0$. That is so because $\langle n \rangle_h$ is calculated from the normalized P_n^h, and can be large even if there is rarely a jet event. It is unfortunate that we cannot compare our results with the multiplicities, $\langle n \rangle_{\text{no jet}}$ and $\langle n \rangle_{\text{jet}}$, determined in the UA1 experiment,[3] since our separation into the soft and hard components bears no relationship to the *ad hoc* separation into the no-jet and jet events in that experiment.

By virtue of the good agreement of our results with the data on C_q in Fig. 6, we have succeeded in demonstrating

that the GBM with jets can readily explain the violation of KNO scaling in the $S\bar{p}pS$ energy range. With the moments being so well specified by our model, it should not be a surprise that we can generate a spectacular fit of the full multiplicity distribution at any energy. An example at 540 GeV is shown in Fig. 7 (Ref. 18) in which we also exhibit the contributions from the soft and hard components separately. It is important to recognize that the soft component in Fig. 7 is not the KNO-scaling curve of Fig. 3 in Ref. 1 because the $\langle n \rangle$ used in both the abscissa and ordinate in the plot in Fig. 7 includes $\langle n \rangle_h$, which is sizable compared to $\langle n \rangle_s$, as can be seen in Fig. 5. Furthermore, $\sigma^h/\sigma_{\text{in}}$ in (3.4) is not negligible.

It is a prediction of the model that the broadening will continue with increasing s. The broadening studied in this paper is due to the appearance of the hard components with high multiplicity. As s is increased to even higher values, jet production will be so dominant that the soft cross section will become vanishingly small on account of the $\exp(-2\Omega_1)$ factor in (2.3). Then the two-component description turns back to essentially only one component, albeit a different one. However, the multiplicity distribution should continue to broaden. The reason is that virtuality smearing, which is the new source of fluctuation, will cover a wider range at higher s. Besides, multijet processes will become increasingly more important.

A final point to note here is that in our approximation for the initial-state bremsstrahlung we have $\langle m \rangle_h = \langle j \rangle_h$, which is about $\frac{1}{3}$ of $\langle l \rangle_h$, as can be read off from Fig. 5. Since $\langle l \rangle_h$ is about $\frac{10}{9}$ of $\langle n \rangle_s$, it means that $\langle l \rangle_h + \langle m \rangle_h$ is about $1.4\langle n \rangle_s$. A more realistic treatment of the bremsstrahlung process may well increase $\langle m \rangle_h$ and decrease $\langle j \rangle_h$, which would further raise $\langle l \rangle_h + \langle m \rangle_h$ compared to $\langle n \rangle_s$. Since the bremsstrahlung products are distributed over all pseudorapidities, $\langle l \rangle_h + \langle m \rangle_h$ contributes to the background in $dE_T/d\eta$, above which jet particles would contribute to a peak. Thus large $\langle l \rangle_h + \langle m \rangle_h$ compared to $\langle n \rangle_s$ implies that in the $dE_T/d\eta$ vs η plot the background associated with the jets is significantly higher than the minimum-bias plateaus. This has come to be known as the pedestal effect, and has been seen in the UA1 data.[3]

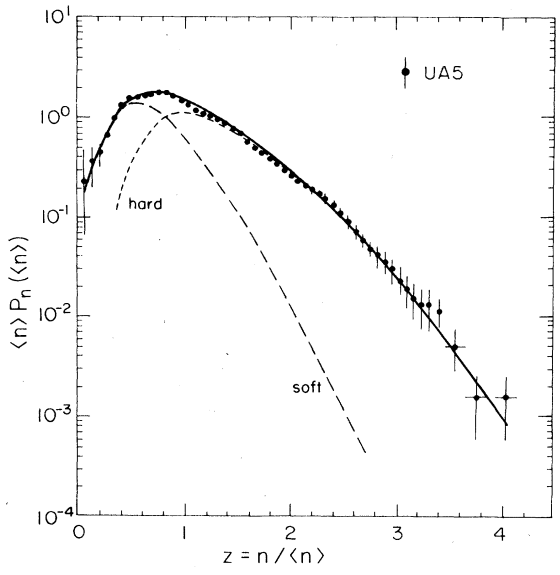

FIG. 7. A KNO plot of multiplicity distribution at $\sqrt{s} = 540$ GeV. The solid line corresponds to the P_n calculated from (3.4); the dashed and dotted lines are the soft and hard components, calculated from P_n^s and P_n^h, respectively. Data points are from Ref. 18.

IV. CONCLUSION

We have successfully shown that our geometrical model for hadronic collisions can describe all prominent features observed in the laboratory. The model is framed in the eikonal formalism, uses Furry branching to describe soft production, incorporates perturbative QCD to describe hard subprocesses, and relies on the geometrical scaling to define the soft component when the production of jets is not negligible. It integrates the studies of elastic scattering, total cross section, multiplicity distributions, correlations, and jet production. In this paper we have concentrated on the confrontation of the data with the model and showed most importantly that our conception of the soft and hard components is phenomenologically sensible.

In order to avoid any arbitrariness in the definition of a jet, we used geometrical scaling extended to the energy region where $\sigma_{\text{el}}/\sigma_{\text{tot}}$ is not constant to define the soft component subject to unitarity correction. The hard component is then expressed in terms of a σ_{jet} without the prior definition of what a jet is. The fact that we later relate σ_{jet} to a $k_T^{\min}$ in perturbative QCD is secondary to our procedure for the soft-hard separation. Thus as far as the separation into soft and hard components is concerned, we need not deal with an *ad hoc* cutoff either to justify the validity of the perturbation theory or to facilitate experimental identifications, both of which involve limitations that are not inherent parts of the physics of multiparticle production.

The value of 2.7 GeV for $k_T^{\min}$ is in the middle of the grey region from 1 to 4 GeV, in the sense that below 1 GeV all processes can reasonably be classified as soft, whereas above 4 GeV the perturbative results in QCD can most probably be trusted. The specific value of 2.7 GeV (which is fortunately within that range) has no special significance apart from indicating that the hard component that breaks geometrical scaling as well as KNO scaling is large, and that the same value for $k_T^{\min}$ suffices for all energies where jets are produced. A concomitant result in our analysis is that the geometrical cross section σ_0 becomes constant above 200 GeV. An explicit experimental verification of this result would be of great interest.

We have also shown that the moments of the multiplicity distribution of the GBM with jets can be made to agree very well with the UA5 data. Because of unknowns in the particle production processes in the hard component, parametrization of $\bar{j}(\hat{Q}^2)$ and $N(s)$ have to be adjusted. We do not regard this as a serious drawback.

At this point our aim is to construct a framework in which all prominent features of hadronic collisions over a wide range of energy can be the natural consequences in the model. As we learn more about this framework, we hope to approach a level of understanding whereby those consequences can become inevitable.

We believe that this framework is now firm enough to warrant further extension into the area of rapidity and p_T distributions of the produced particles. An investigation of the rapidity-interval dependence of the multiplicity distribution has already been considered.[19] The multiplicity dependence of $\langle p_T \rangle$ is found to have an interesting "ledge" effect.[20] We feel that the geometrical branching model is in the hub of a multiply connected scheme which shares common grounds with many otherwise disconnected views about hadronic collisions, as in the simple geometrical model, parton model, statistical model, dual topological model, branching model, string model, etc. It would indeed be a worthy goal if in the end a unified picture of all those views can emerge.

ACKNOWLEDGMENT

This work was supported in part by the U.S. Department of Energy under Grant No. DE-FG06-85ER40224-A001.

[1]W. R. Chen and R. C. Hwa, Phys. Rev. D **36**, 760 (1987).

[2]R. C. Hwa, Phys. Rev. D **37**, 1830 (1988). Equations in this paper will be referred to with a prefix II.

[3]G. Piano Mortari, in *Proceedings of the Oregon Meeting,* Annual Meeting of the Division of Particles and Fields of the APS, Eugene, Oregon, 1985, edited by R. C. Hwa (World Scientific, Singapore, 1986), p. 615.

[4]L. Durand and H. Pi, Phys. Rev. Lett. **58**, 303 (1987).

[5]J. Dias de Deus, Nucl. Phys. **B59**, 231 (1973); A. J. Buras and J. Dias de Deus, *ibid.* **B71**, 481 (1974).

[6]A. W. Chao and C. N. Yang, Phys. Rev. D **8**, 2063 (1973).

[7]U. Amaldi and K. R. Schubert, Nucl. Phys. **B166**, 301 (1980).

[8]UA4 Collaboration, M. Bozzo *et al.*, Phys. Lett. **147B**, 392 (1984).

[9]UA5 Collaboration, P. Carlson, in *Proceedings of the Oregon Meeting* (Ref. 3), p. 680.

[10]F. Halzen and P. Hoyer, Phys. Lett. **130B**, 326 (1983).

[11]G. Pancheri and Y. N. Srivastava, Phys. Lett. B **182**, 199 (1986).

[12]A. Norton, in *Multiparticle Production,* proceedings of the Shandong Workshop, Jinan, China, 1987, edited by R. C. Hwa and Q. B. Xie (World Scientific, Singapore, 1988).

[13]M. Derrick *et al.*, Phys. Lett. **168B**, 299 (1986).

[14]The coefficient of $N(s)$ in (3.21) was previously in the range 0.1–0.145 in Ref. 1. In this paper we have used the improved forms for $\Omega_0(R)$ [see (2.10)] and $h(R)$ [see (3.23)], thus resulting in the value 0.114.

[15]W. R. Chen, R. C. Hwa, and X.-N. Wang, Phys. Rev. D **38**, 3394 (1988).

[16]UA5 Collaboration, G. J. Alner *et al.*, Phys. Lett. **160B**, 199 (1985); **167B**, 476 (1986).

[17]This formula would not be affected in any significant way, if energy conservation is taken into account in the calculation of the s dependence of the soft component of the average multiplicity in the hard process by subtracting out the energy for jet production. We have calculated the average momentum fraction $\langle x_1 x_2 \rangle$ using the weight expressed in (2.13). It is very small, ranging from 0.004 to 0.001 at the CERN collider energies. Thus the residual energy available for soft production in a process with jets is $[(1-\langle x_1 x_2 \rangle)s]^{1/2} \approx \sqrt{s}$.

[18]UA5 Collaboration, G. J. Alner *et al.*, Phys. Lett. **138B**, 304 (1984).

[19]R. C. Hwa, Phys. Rev. D **37**, 2451 (1988).

[20]X.-N. Wang and R. C. Hwa, following paper, Phys. Rev. D **39**, 187 (1989).